Journal of Applied Fluid Mechanics, Vol. 12, No. 5, pp. 1439-1447, 2019.
Available online at www.jafmonline.net, ISSN 1735-3572, EISSN 1735-3645.
DOI: 10.29252/jafm.12.05.29533

Experimental Study on the Discharge Coefficient of Bi-Swirl Coaxial Injectors

K. Ahn[1†] and B. J. Lee[2]

[1] *School of Mechanical Engineering, Chungbuk National University, 1 Chungdae-ro, Seowon-gu, Cheongju, Chungbuk 28644, Korea*
[2] *Department of Mechanical and Aerospace Engineering, Seoul National University, 1 Gwanak-ro, Gwanak-gu, Seoul 08826, Korea*

†*Corresponding Author Email: kbahn@cbnu.ac.kr*

(Received August 14, 2018; accepted December 16, 2018)

ABSTRACT

An experimental study was carried out to investigate the effects of recess length and mixture ratio on the discharge coefficient of bi-swirl coaxial injectors with inner closed-type and outer open-type swirl injectors. Ten bi-swirl coaxial injectors were classified into two groups with different recess lengths. By independently varying the mass flow rates through the inner and outer injectors, the discharge coefficients of the injectors were obtained. Single-injection cold-flow tests indicated that the discharge coefficients of both the inner and outer swirl injectors were only marginally affected by the recess length and mass flow rate. Bi-injection cold-flow tests showed that the discharge coefficients of the inner swirl injectors were also almost constant, regardless of the recess length and mixture ratio. On the other hand, those of the outer swirl injectors in the tip-mixing and internal-mixing bi-swirl coaxial injectors with long recess lengths had significantly decreased with the increase in mixture ratio. A novel empirical equation for the discharge coefficient of the outer swirl injector in the internal-mixing bi-swirl coaxial injector is suggested through a linear regression analysis of the present test data. It was found that the present empirical equation could accurately predict the experimental data.

Keywords: Bi-swirl coaxial injector; Discharge coefficient; Recess length; Mixture ratio; Liquid rocket engine.

NOMENCLATURE

a	constant
A	area
Cd	discharge coefficient
d	diameter
K	swirl injector geometric constant,
l_C	distance between the inner swirl injector nozzle tip and the colliding point of the inner liquid sheet on the outer swirl injector nozzle wall
l_R	recess length
m	mass flow rate
MR	ratio of the inner mass flow rate to the outer mass flow rate
n	number of tangential holes
r	radius
R	radial distance from the center of theinjector to the center of the tangential hole
R_{Cd}	ratio of the discharge coefficient under bi-injection to the discharge coefficient under single-injection
$R_{\Delta P}$	ratio of the injection pressure drop through the inner swirl injector to the injection pressure drop through the outer swirl injector under single-injection corresponding to the inner and outer mass flow rates under bi-injection respectively
RN	recess number
α	exponent
β	exponent
ΔP	injection pressure drop
ρ	fluid density

SUBSCRIPTS

B	bi-injection
h	tangential hole
I	inner swirl injector
mea	measured from the present cold-flow test
n	nozzle
O	outer swirl injector
s	swirl chamber
S	single-injection

1. INTRODUCTION

A liquid rocket engine (LRE) employs injectors to disintegrate propellants into small droplets which are then efficiently mixed. Several different types of injectors (impinging, coaxial, pintle, etc.) have been adopted in LREs (Gill and Nurick, 1976). Coaxial-type injectors include shear coaxial, swirl coaxial, and bi-swirl coaxial injectors, which are selected according to the propellants and their phases (Ahn *et al.*, 2011; Im *et al.*, 2010; Locke *et al.*, 2010). The bi-swirl coaxial injector consists of inner and outer swirl injectors as one body, and discharges generally liquid-phase propellants such as liquid oxygen (LOx) and kerosene into a combustion chamber.

Before designing the bi-swirl coaxial injector for a LRE, the property of the propellant (density, viscosity, etc.), mass flow rate, and pressure drop through each injector are pre-specified. The injection pressure drop should exceed at least 8% of the chamber pressure to avoid low-frequency combustion instability, and is typically 15% to 20% of the chamber pressure to facilitate the management of the pump requirements (Greene *et al.*, 2002; Huzel and Huang, 1992; Smith *et al.*, 2004). To make the best use of the allowable pressure drop for good atomization and mixing, the discharge coefficient of the injector must be predictable. The inner and outer swirl injector of the bi-swirl coaxial injector can be closed-type, open-type, or screw-type (Ahn and Choi 2017a, b; Gotzig and Dargies, 2003). Accordingly, the bi-swirl coaxial injector follows the general swirl injector design.

Many researchers have studied the discharge coefficient of closed-type swirl injectors and have suggested their empirical equations (Ballester and Dopazo, 1994; Bayvel and Orzechowski, 1993; Bazarov *et al.*, 2004; Jones, 1982; Rizk and Lefebvre, 1985; Taylor, 1950). While the swirl chamber diameter of the closed-type swirl injector is larger than the nozzle diameter, the swirl chamber diameter of the open-type swirl injector is equal to the nozzle diameter. A few studies have been performed on the discharge coefficient of open-type swirl injectors (Fu *et al.*, 2012; Hong *et al.*, 2012). Regardless of the swirl injector type, each of these studies emphasized the importance of the swirl injector geometric constant (K) or the atomizer constant on the discharge coefficient. By conducting cold-flow tests on several dozens of closed-type and open-type swirl injectors, Ahn and Choi (2017a, b) proposed empirical equations as a function of the swirl injector geometric constant. They also confirmed that the design method for the closed-type swirl injector reported by Bazarov *et al.* (2004) and its modified version for the open-type swirl injector could effectively predict the discharge coefficient of the swirl injector within the injector geometries and experimental conditions.

Recent hot-firing tests using bi-swirl coaxial injectors in LOx/kerosene LRE thrust chambers and gas generators showed that the discharge coefficients under hot-firing tests were reduced compared to those under cold-flow tests (Ahn and Choi 2012a; Ahn *et al.*, 2012b). Similar to the behavior of the recess in the shear coaxial injector (Candel *et al.*, 2006; Kendrick *et al.*, 1999; Lux and Haidn, 2009), the increase of recess length in the bi-swirl coaxial injectors of the same shape caused a decrease in the discharge coefficients of both the inner and outer injectors. As the mixture ratio increased, the discharge coefficients of the outer swirl injectors decreased. It is believed that the flame anchored inside the recessed region in the bi-swirl coaxial injectors confined flows of LOx and kerosene, and the collision of LOx sheet with the fuel film on the outer injector nozzle partially blocked the flow of the fuel film. Although the two factors apparently affected the change in discharge coefficients, the extent of each effect could not be quantitatively distinguished.

In this study, five bi-swirl coaxial injectors with different recess lengths for a thrust chamber and the other five bi-swirl coaxial injectors with different recess lengths for a gas generator were designed and manufactured. By changing the inner and outer mass flow rates through each bi-swirl coaxial injector, hydraulic cold-flow tests were conducted using tap water to measure the discharge coefficient. The effects of recess length, mixture ratio, and injector geometry on the variation of the discharge coefficient were investigated. A simple empirical equation for the discharge coefficient of the outer swirl injector in the internal-mixing bi-swirl coaxial injector under bi-injection is suggested from the present experimental data.

2. EXPERIMENTAL METHODS

2.1 Bi-Swirl Coaxial Injectors and Experimental Setup

A schematic of the bi-swirl coaxial injectors used in the present study is illustrated in Fig. 1. The bi-swirl coaxial injectors have an inner closed-type swirl injector ($d_s > d_n$) for LOx and an outer open-type swirl injector ($d_s = d_n$) for kerosene. Two groups of injectors were designed and fabricated. Five bi-swirl coaxial injectors (Inj#1 model) with different recess lengths of from 0.0 to 6.0 mm for a thrust chamber and five bi-swirl coaxial injectors (Inj#2 model) with recess lengths of from 0.0 to 5.0 mm for a gas generator are very similar to the injectors used by Ahn *et al.* (2014) and Ahn and Choi (2012a), respectively. The swirl directions of both the inner and outer swirl injectors are clockwise to the nozzle.

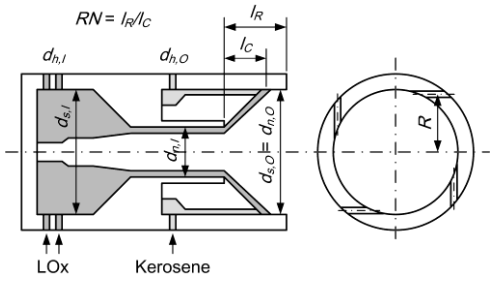

Fig. 1. Schematic of the present bi-swirl coaxial injector.

Table 1 Geometric information on the present bi-swirl coaxial injectors

Injector model	Unit	Inj#1					Inj#2				
		Inner closed-type			Outer open-type		Inner closed-type			Outer open-type	
K		0.98			16.48		0.91			2.50	
n_h	mm	8			4		3			4	
d_h		1.48			0.86		1.10			1.20	
d_s		6.7			7.5		3.5			4.5	
d_n		3.5			7.5		1.5			4.5	
R		2.45			3.25		1.10			1.60	
l_R	mm	0.0	1.9	3.6	4.5	6.0	0.0	1.4	2.6	3.8	5.0
RN		0.00	0.53	1.00	1.25	1.66	0.00	0.50	0.92	1.35	1.77

Detailed geometric information on the present injectors is summarized in Table 1. The recess number (RN) is defined as a dimensionless parameter, $RN = l_R/l_C$, which divides the recess length (l_R) by the distance between the oxidizer post tip and the colliding point of the oxidizer sheet into the fuel nozzle wall (l_C). Here, l_C was calculated from the injector geometric dimensions and the average spray cone angle measured through cold-flow tests in the injectors with l_R = 0.0 mm (Ahn *et al.*, 2011; Ahn *et al.*, 2014). l_C was 3.61 mm and 2.82 mm for the Inj#1 and the Inj#2 models, respectively. According to the recess number, the bi-swirl coaxial injector has external-mixing (RN < 1), tip-mixing ($RN \approx 1$), and internal-mixing characteristics (RN > 1) (Ahn *et al.*, 2012b; Kim, 2007). Each injector group thus has two external-mixing, one tip-mixing, and two internal-mixing injectors. In the case of RN < 1, the inner and outer liquid sheets do not mix inside the bi-swirl coaxial injector. On the contrary, in the case of RN > 1, the inner liquid sheet collides with the outer liquid film on the outer injector wall and the two liquids are mixed inside the injector.

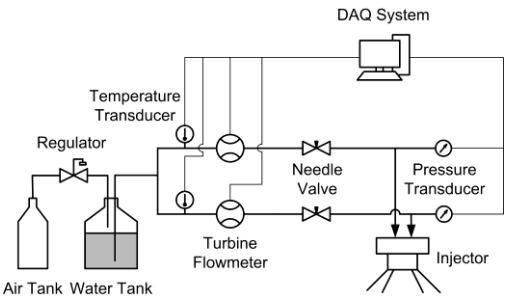

Fig. 2. Experimental setup for cold-flow tests of bi-swirl coaxial injectors.

The present experimental setup is explained in Fig. 2. Tap water was used as a liquid simulant instead of LOx and kerosene. The water in the tank, which was pressurized by a regulator connected to a compressed air bottle, was controlled and supplied into each manifold of the bi-swirl coaxial injector by needle valves. A turbine flow meter (Kometer, NK-250) and a K-type thermocouple were installed in each supply line to measure the mass flow rate, and a pressure transducer (Sensys, PSH model) was located in each manifold to directly gauge the injection pressure. Data detected from these sensors was recorded by a NI c-DAQ at a rate of 1 kHz for 1 second. The temperature of the tap water was approximately 285 K. The density, dynamic viscosity, and surface tension of the water were estimated to be 999.5 kg/m3, 1239.2 μPa·s, and 74.0 mN/m, respectively.

2.2 Experimental Conditions

Figure 3 shows the experimental conditions as a function of the inner and outer mass flow rate for the Inj#1 and Inj#2 models. Here, DP (m_I = 162.21 g/s, m_O = 57.93 g/s for Inj#1 models and m_I = 28.92 g/s, m_O = 90.00 g/s for Inj#2 models) is the nominal operating condition and the ODs are off-nominal operating conditions that have ± 20% mass flow rate deviations based on DP. The Inj#1 injectors are designed for a liquid rocket engine thrust chamber using LOx through the inner swirl injector and Jet A-1 through the outer swirl injector. Therefore, the inner mass flow rate was higher than the outer mass flow rate. The mixture ratio (MR) of the inner mass flow rate to the outer mass flow rate was varied from 1.87 to 4.20. On the other hand, the Inj#2 injectors are designed for a liquid rocket engine gas generator using the same propellants. Thus, the inner mass flow rate for the Inj#2 injectors was less than that of the outer mass flow rate, and MR ranged from 0.21 to 0.48. Cold-flow tests for each condition were conducted under single-injection and bi-injection, and were repeated twice.

3. Experimental Results

3.1 Discharge Coefficient under Single-Injection

Injection pressure drop data under single-injection for all the injectors are plotted in Fig. 4 as a function of the mass flow rate. The injection pressure drop through the inner or outer swirl injector quadratically increased with the increment of the inner or outer mass flow rate. The variation in recess length did not significantly affect the pressure drop of the bi-swirl coaxial injectors under single-injection. The injection pressure drop was between 4 bar and 16 bar within the whole range of test conditions.

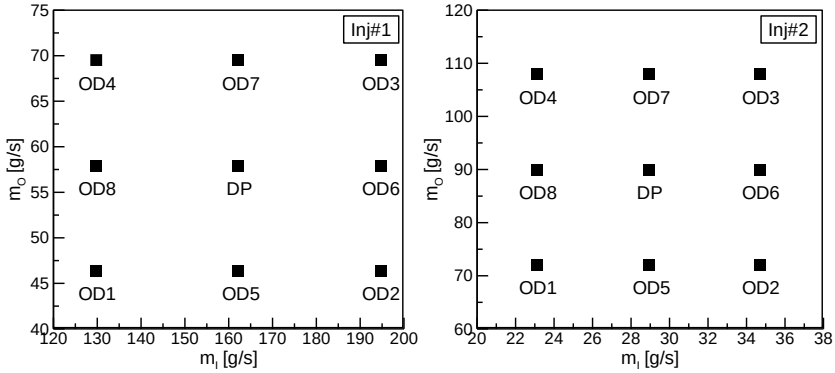

Fig. 3. Experimental conditions as a function of the inner and outer mass flow rates.

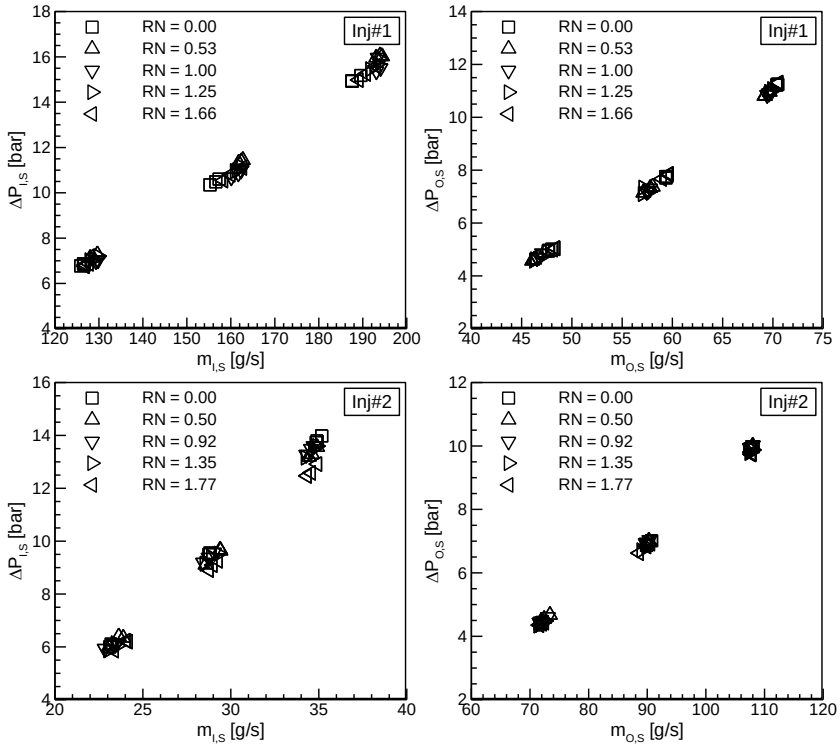

Fig. 4. Injection pressure drop data according to the mass flow rate under single-injection.

The discharge coefficient of an injector is defined as follows:

$$Cd = \frac{m}{A_n \sqrt{2\rho\Delta P}} \tag{1}$$

Since the swirl injector has a gas core inside the injector due to the centrifugal force of liquid, it has a very low discharge coefficient compared to other injector types. The discharge coefficient was calculated from the present measurement data under single-injection and is plotted in Fig. 5 according to the mass flow rate. The discharge coefficient for each injector was almost constant since the spray of the swirl injectors was fully developed due to a sufficient injection pressure drop. As can be anticipated from Fig. 4, the recess length hardly influenced the discharge coefficient of the bi-swirl coaxial injectors under single-injection. The maximum deviation in the discharge coefficient data was less than 3%, irrespective of the mass flow rate and recess length. Since the *K* value of the outer swirl injectors for the Inj#1 models was the largest, their discharge coefficient data were the smallest.

Bazarov *et al.* (2004) published a complex model to accurately predict the discharge coefficient of the closed-type swirl injector. Ahn and Choi (2017a) verified the model by comparing it with their experimental data. Ahn and Choi (2017b) simplified the model to apply it to the open-type swirl injector and validated the modified model with their experimental data. The discharge coefficient, which was calculated from the models of Bazarov *et al.* (2004) for the closed-type swirl injector and Ahn and Choi (2017b) for the open-type swirl injector, is represented by a dashed line in Fig. 5. The measured discharge coefficient data were approximately the same as the predicted values. Therefore, if the geometry of a swirl injector and liquid properties are

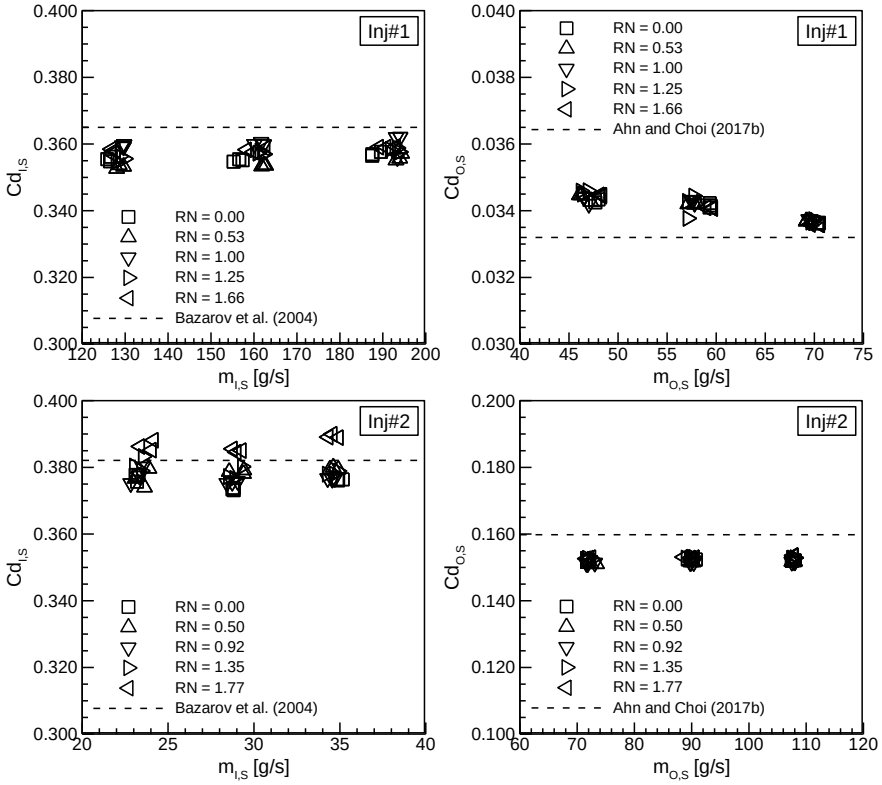

Fig. 5. Discharge coefficient data according to the mass flow rate under single-injection.

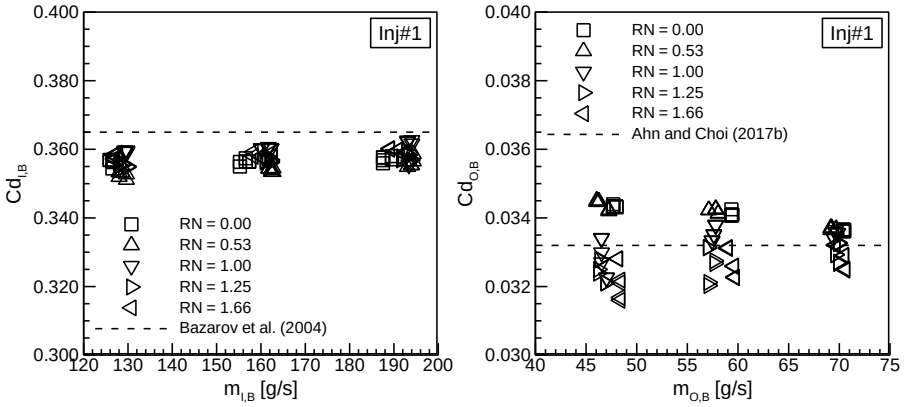

Fig. 6. Discharge coefficient data for the Inj#1 injectors according to the mass flow rate under bi-injection.

known, it is possible to estimate the injection pressure drop of the swirl injector at a given mass flow rate.

3.2 Discharge Coefficient under Bi-Injection

Figure 6 shows the discharge coefficient data under bi-injection for the Inj#1 injectors. Compared with the results in Fig. 5, the discharge coefficient data through the inner swirl injector of the Inj#1 injectors under bi-injection closely matched those under single-injection, regardless of recess length. The discharge coefficient data through the outer swirl injector of the Inj#1 injectors with $RN < 1$ under bi-injection were also consistent with those under single-injection. On the other hand, the discharge coefficient values through the outer swirl injector of the Inj#1 injectors with $RN > 1$ were distinctly lower than those under single-injection, although the increase of the outer mass flow rate resulted in the gradual recovery of the discharge coefficient values.

To investigate the effect of recess length and bi-injection on the variation in discharge coefficient, the ratio of the discharge coefficient under bi-injection to that under single-injection (R_{Cd}) corresponding to the same mass flow rate was calculated and is plotted in Fig. 7 as a function of *MR*. Since the test conditions were based on the mass flow rates, a R_{Cd} of 1 implies no difference between the single-injection and bi-injection. A R_{Cd} of less than 1 implies that more pressure drop is required to discharge the same mass flow rate under bi-injection.

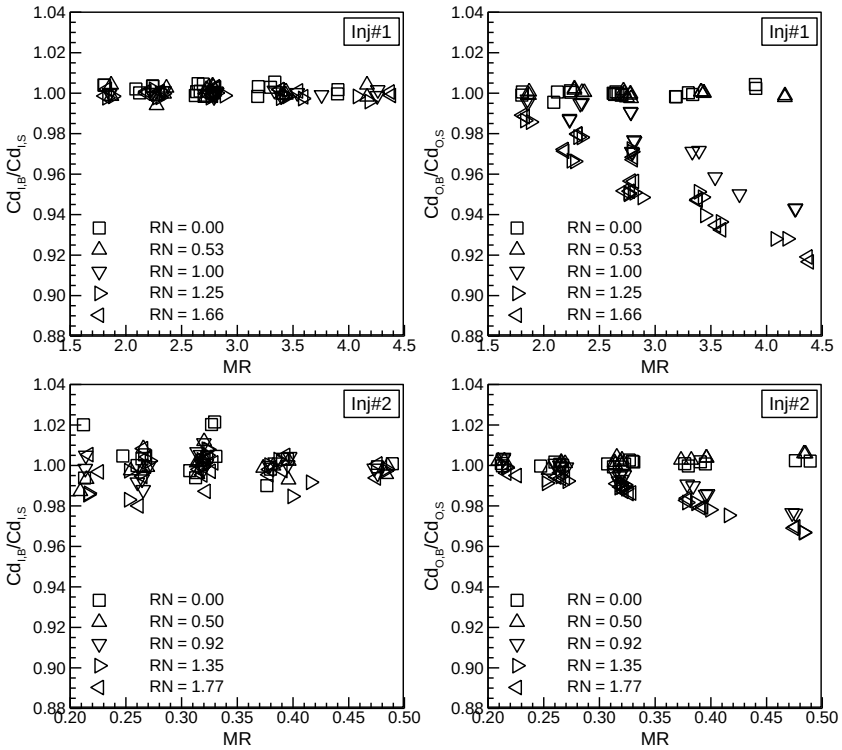

Fig. 7. Ratio of the discharge coefficient under bi-injection to that under single-injection as a function of mixture ratio.

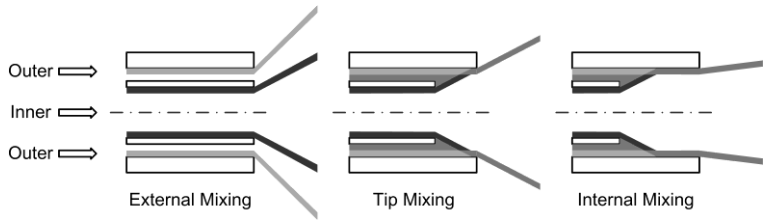

Fig. 8. Schematic of flow patterns in external-mixing, tip-mixing, and internal-mixing bi-swirl coaxial injectors.

Regardless of the recess length and mixture ratio, the R_{Cd} through the inner swirl injector of all the bi-swirl coaxial injectors was almost 1.00. This means that bi-injection did not affect the discharge coefficient of the inner swirl injector. The R_{Cd} through the outer swirl injector of the bi-swirl coaxial injectors with $RN < 0.90$ was nearly 1.00, while that with $RN > 0.90$ decreased with the increment of the mixture ratio. The decrease in the R_{Cd} with $RN > 1.00$ was greater than that with $RN \approx 1.00$. Although the quantitative amount of the decrease differs, the present tendency agrees with the results in the hot-firing tests (Ahn and Choi, 2012a; Ahn *et al.*, 2012b).

The reason for this is illustrated in Fig. 8, which shows a schematic of flow patterns in the external-mixing, tip-mixing, and internal-mixing bi-swirl coaxial injectors obtained from numerical results (Lee *et al.*, 2017; Lee *et al.*, 2018). In the case of the external-mixing bi-swirl coaxial injector, two liquid sheets are discharged without affecting each other, similar to the liquid sheet under single-injection. On the other hand, in the case of the internal-mixing injector, the space between the inner swirl injector nozzle and the outer swirl injector nozzle is filled with liquid due to the collision of the inner liquid sheet with the outer liquid film. Thus, the liquid through the outer swirl injector suffers additional frictional loss, which causes an increased pressure drop of the outer liquid at a fixed mass flow rate. As the *MR* increases, the collision force increases and the outer liquid experiences increased blocking force. At the same *MR*, the R_{Cd} through the outer swirl injector of the tip-mixing injector was greater than that of the internal-mixing injector because a portion of the inner liquid sheet collided with the outer liquid film in the tip-mixing bi-swirl coaxial injector.

The effect of the inner mass flow rate and the outer mass flow rate on the R_{Cd} for the outer swirl injector of the Inj#1 injector with $RN = 1.66$ is illustrated in Fig. 9. The increase of the inner mass flow rate at the same outer mass flow rate resulted in a decrease in the R_{Cd}, while the R_{Cd} increased due to the increase of the outer mass flow rate at the same inner mass flow rate. However, the R_{Cd} was not constant at the same mixture ratio, and slightly increased with the increment of total mass flow rate. This implies that the R_{Cd} is not a function of only the mixture ratio.

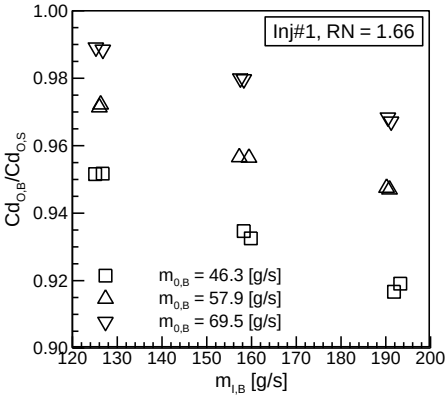

Fig. 9. Ratio of the discharge coefficient through the outer swirl injector under bi-injection to that under single-injection according to the inner and outer mass flow rates.

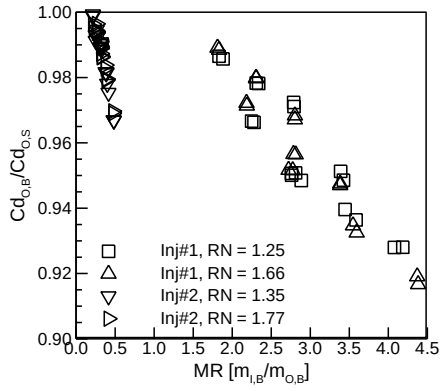

(a)

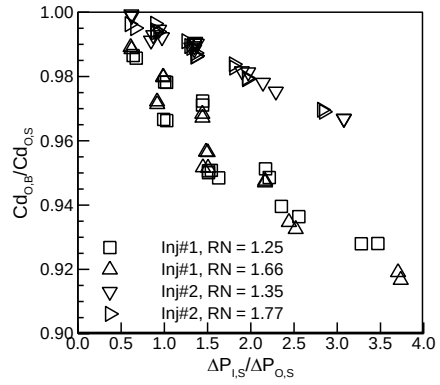

(b)

Fig. 10. Ratio of the discharge coefficient through the outer swirl injector under bi-injection to that under single-injection in the internal-mixing bi-swirl coaxial injectors.

3.3 R_{Cd} of the Outer Injector in the Internal-Mixing bi-Swirl Coaxial Injector

Figure 10(a) shows the R_{Cd} data for the outer swirl injector of the bi-swirl coaxial injectors with RN > 1.00 as a function of MR. While the mixture ratio influenced the variation of R_{Cd}, the fitting trends for the Inj#1 and Inj#2 injectors differed. As the MR increases, the slope of the R_{Cd} of the Inj#2 injectors declined more steeply than that of the Inj#1 injectors. The R_{Cd} data are again plotted in Fig. 10(b) as a function of the ratio of the inner injection pressure drop under single-injection to the outer injection pressure drop under single-injection ($R_{\Delta P}$) corresponding to the inner and outer mass flow rates under bi-injection, respectively. The R_{Cd} decreased almost linearly with respect to the $R_{\Delta P}$, but the reduction slope of the Inj#1 injectors was greater than that of the Inj#2 injectors. Although the mixture ratio and the $R_{\Delta P}$ affected the R_{Cd}, the extent of each effect was dependent on the injector geometry.

If the mixture ratio or the $R_{\Delta P}$ reaches 0, the influence of bi-injection on the internal-mixing bi-swirl coaxial injector would disappear, and the following assumption can thus be made.

$$Cd_{O,B}/Cd_{O,S} = 1 - a \times MR^{\alpha} \times R_{\Delta P}^{\beta} \quad (2)$$

The following empirical equation consisting of MR and $R_{\Delta P}$ was therefore obtained through a linear least-squares regression analysis which minimizes the sum of the squares of the residual errors for all the available data (Chapra, 2012).

$$Cd_{O,B}/Cd_{O,S} = 1 - 0.01846 \times MR^{0.4559} \times R_{\Delta P}^{0.6601} \quad (3)$$

In Fig. 11, the experimental results are compared with those calculated from Eq. (3). The deviation is distributed between -1.0% and 1.2% within the present experimental range, irrespective of the Inj#1 and Inj#2 injectors.

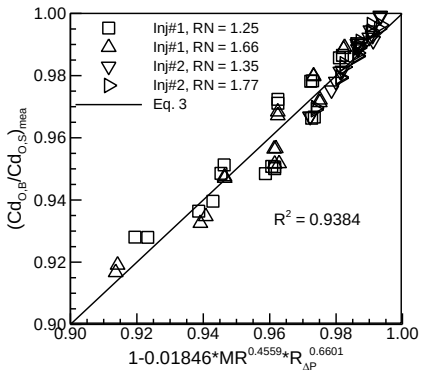

Fig. 11. Comparison between the R_{Cd} data measured from the present experiments and those calculated from Eq. (3).

4. CONCLUSION

Research on ten bi-swirl coaxial injectors was performed to investigate the discharge coefficient with respect to the overall injector size, recess length, and mixture ratio. The discharge coefficients under single-injection and bi-injection were experimentally studied.

Single-injection cold-flow tests confirmed that the discharge coefficients for both the inner and outer swirl injectors did not significantly change irrespective of the recess length and mass flow rate. Bi-injection cold-flow tests showed that the discharge coefficients of the inner swirl injector in the bi-swirl coaxial injectors and those of the outer

swirl injector in the external-mixing bi-swirl coaxial injectors were unaffected by the recess length and mixture ratio. On the other hand, the discharge coefficients of the outer swirl injector in the tip-mixing and internal-mixing bi-swirl coaxial injectors significantly decreased with the increase in the mixture ratio.

For the discharge coefficient of the outer swirl injector in the internal-mixing bi-swirl coaxial injector, a novel empirical equation as a function of the MR and $R_{\Delta P}$ is suggested. The empirical equation closely matched the experimental data. Since MR and $R_{\Delta P}$ can be calculated from the geometry of the designed bi-swirl coaxial injector, the mass flow rates of the propellants, and the empirical equations for the discharge coefficients of the closed-type (Ahn and Choi, 2017a; Bazarov *et al.*, 2004) and open-type swirl injectors (Ahn and Choi 2017b), one can predict the discharge coefficient of the outer swirl injector in the internal-mixing bi-swirl coaxial injector from Eq. (3).

The aim of the present study was to address the problem of the reduction of the discharge coefficients in hot-firing tests compared to those in single-injection cold-flow tests (Ahn and Choi, 2012a; Ahn *et al.*, 2012b). The hot-firing tests showed that the decrease in the discharge coefficients of the inner swirl injectors with the increase in recess length differed from that of the present cold-flow results, and the discharge coefficients of the outer swirl injectors were more reduced than those in the present cold-flow tests. It is therefore possible to distinguish the effects of the fluid collision and the flame anchoring inside the recessed region on the discharge coefficient of the bi-swirl coaxial injector.

The present injectors use LOx and kerosene in liquid rocket engine combustion devices. The properties (density, viscosity, surface tension, etc.) of LOx and kerosene are different from those of tap water at room temperature. The suggested empirical equation appears to be applicable to other fluid types because it is dimensionless, but the difference in density between LOx and kerosene is not considered in the equation. Therefore, if two different fluids are used, the suggested empirical equation must be carefully applied. The research using two different fluids to enhance this study is highly recommended.

ACKNOWLEDGEMENTS

This research was supported by National Research Foundation grants (NRF-2013R1A5A1073861, NRF-2017R1A1A1A05001237, and NRF-2018M1A3A3A02065683), funded by the Ministry of Science and ICT, South Korea. The authors would like to thank the MSIT for its support.

REFERENCES

Ahn, K. and H. S. Choi (2012a). Combustion dynamics of swirl coaxial injectors in fuel-rich combustion. *Journal of Propulsion and Power* 28(6), 1359-1367.

Ahn, K. and H. S. Choi (2017a). A study on discharge coefficients of closed-type swirl injectors for a liquid rocket engine. *Atomization and Sprays* 27(7), 569-578.

Ahn, K. and H. S. Choi (2017b). An extensive study on the discharge coefficients of open-type swirl injectors. *Atomization and Sprays* 27(10), 835-846.

Ahn, K., J. G. Kim and H. S. Choi (2014). Effects of injector recess on heat flux in a combustion chamber with cooling channels. *Aerospace Science and Technology* 37, 110-116.

Ahn, K., S. Seo and H. S. Choi (2011). Fuel-rich combustion characteristics of biswirl coaxial injectors. *Journal of Propulsion and Power* 27(4), 864-872.

Ahn, K., Y. M. Han and H. S. Choi (2012b). Effects of recess length on discharge coefficients of swirl coaxial injectors. *Combustion Science and Technology* 184(3), 323-336.

Ballester, J. and C. Dopazo (1994). Discharge coefficient and spray angle measurements for small pressure-swirl nozzles. *Atomization and Sprays* 4(3), 351-367.

Bayvel, L. and Z. Orzechowski (1993). *Liquid Atomization*. Taylor & Francis, Washington, D. C., U.S.A.

Bazarov, V., V. Yang and P. Puri (2004). Design and dynamics of jet and swirl injectors. In V. Yang, M. Habiballah, J. Hulka and M. Popp (Ed.), *Liquid Rocket Thrust Chambers: Aspects of Modeling, Analysis, and Design*, Reston, Virginia, U.S.A., 19-103.

Candel, S., M. Juniper, G. Singla, P. Scouflaire and C. Rolon (2006). Structure and dynamics of cryogenic flames at supercritical pressure. *Combustion Science and Technology* 178(1-3), 161-192.

Chapra, S. C. (2012). *Applied Numerical Methods with MATLAB for Engineers and Scientists.* McGraw-Hill, New York, U.S.A.

Fu, Q., L. Yang, W. Zhang and K. Cui (2012). Spray characteristics of an open-end swirl injector. *Atomization and Sprays* 22(5), 431-445.

Gill, G. S. and W. H. Nurick (1976). *Liquid Rocket Engine Injectors*. NASA Rep. SP-8089, U.S.A.

Gotzig, U. and E. Dargies (2003, July). Development status of Astriums New 22N bipropellant thrust family. In *Proceedings of the 39th AIAA/ASME/SAE/ASEE Joint Propulsion Conference and Exhibit*, Huntsville, Alabama, U.S.A.

Greene, C., R. Woodward, S. Pal and R. Santoro (2002, April). Design and study of a LOX/GH_2 throttleable swirl injector for rocket applications. In *Proceedings of the 38th JANNAF Combustion Subcommittee Meeting* 1, Destin, Florida, U.S.A., 479-492.

Hong, M., J. Jeon and S. Y. Lee (2012). Discharge coefficient of pressure-swirl atomizers with low nozzle opening coefficients. *Journal of Propulsion and Power* 28(1), 213-217.

Huzel, D. K. and D. H. Huang (1992). Modern Engineering for Design of Liquid-Propellant Rocket Engines. *Progress in Astronautics and Aeronautics* 147, AIAA, Washington, D.C., U.S.A.

Im, J. H., S. Cho, Y. Yoon and I. Moon (2010). Comparative study of spray characteristics of gas-centered and liquid-centered swirl coaxial injectors. *Journal of Propulsion and Power* 26(6), 1196-1204.

Jones, A. R. (1982, June). Design optimization of a large pressure-jet atomizer for power plant. In *Proceedings of the 2nd International Conference on Liquid Atomization and Spray Systems*, Madison, Wisconsin, U.S.A., 181-185.

Kendrick, D., G. Herding, P. Socuflaire, C. Rolon, and S. Candel (1999). Effects of a recess on cryogenic flame stabilization. *Combustion and Flame* 118(3), 327-339.

Kim, D. (2007). *Spray Characteristics of Swirl Coaxial Type Injectors for Liquid Rocket Engines*. Ph. D. thesis, Seoul National University, Seoul, Korea.

Lee, B., W. Yoon and K. Ahn (2017, October). A CFD study on the spray characteristics of bi-swirl coaxial injector, In *Proceedings of the 19th Annual Conference of ILASS-Asia*, Jeju, Korea.

Lee, B., W. Yoon, Y. Yoon and K. Ahn (2018). Numerical study on swirl coaxial injectors with different recess lengths. *Journal of ILASS-Korea* 23(2), 49-57.

Locke, J. M., S. Pal, R. D. Woodward and R. J. Santoro (2010, July). High speed visualization of LOX/GH_2 injector flowfield: hot-fire and cold-flow experiments. In *Proceedings of the 46th AIAA/ASME/SAE/ASEE Joint Propulsion Conference and Exhibit*, Nashville, Tennessee, U.S.A.

Lux, J. and O. Haidn (2009). Effect of recess in high-pressure liquid oxygen/methane coaxial injection and combustion. *Journal of Propulsion and Power* 25(1), 24-32.

Rizk, N. K. and A. H. Lefebvre (1985). Internal flow characteristics of simplex swirl atomizers. *Journal of Propulsion and Power* 1(3), 193-199.

Smith, J. J., M. Bechle, D. Suslov, M. Oschwald, O. J. Haidn and G. M. Schneider (2004, July). High pressure LOx/H_2 combustion and flame dynamics: preliminary results. In *Proceedings of the 40th AIAA/ASME/SAE/ASEE Joint Propulsion Conference and Exhibit*, Fort Lauderdale, Florida, U.S.A.

Taylor, G. I. (1950). The boundary layer in the converging nozzle of a swirl atomizer. *The Quarterly Journal of Mechanics and Applied Mathematics* 3(2), 129-139.